Wedge-Induced Turbulent Boundary-Layer Separation on a Roughened Surface at Mach 6.0

P. J. Disimile*
University of Cincinnati, Cincinnati, Ohio 45221
and
N. E. Scaggs†
Air Force Wright Research and Development Center, Wright-Patterson Air Force Base, Ohio 45433

Compressible turbulent boundary-layer characteristics on a roughened surface were studied in the presence of a wedge-induced adverse pressure gradient. All tests were conducted at nominal Mach and unit Reynolds numbers of 33 × 10^6, 66 × 10^6, and 98 × 10^6/m. Documentation of the surface pressure distribution confirmed the two dimensionality of the boundary-level flow throughout the interaction region. A 10% change in the upstream extent of the separation point was observed when the Reynolds number was increased from 33 × 10^6 to 66 × 10^6/m. Pitot pressure and total temperature profiles in the boundary layer upstream and downstream of the interaction region were also acquired. Pitot pressure profiles on the ramp were found to reach a maximum 3.5 times that of the local boundary-layer edge pitot pressure. Similarly, total temperature profiles were found to overshoot the stagnation temperature. Furthermore, the bimodal character of these temperature profiles was observed on the ramp with peak values 5–30% larger than the freestream total temperature.

Nomenclature

c = local speed of sound, m/s
M = Mach number
P_i = surface pressure at a given xy location, mm Hg
P_{ref} = undisturbed reference surface pressure acquired at $x = -16.469$ cm, mm Hg
P_s = static pressure, mm Hg
P_t = local pitot pressure, MPa
P_0 = stagnation/reservoir pressure, MPa
Re = unit Reynolds number/m
T_s = static temperature, K
T_t = local total temperature, K
T_0 = stagnation/reservoir temperature
U = local mean velocity, m/s
U_{inf} = freestream velocity, m/s
x = streamwise distance, cm
x_s = separation distance measured from flat plate/wedge intersection point, cm
y = lateral distance along the width of the plate, cm
z = distance taken perpendicular (transverse) to the plate, mm
δ = boundary-layer thickness location where velocity is 99% of freestream, mm

Introduction

A RECENT review of aerothermodynamic problems surrounding hypersonic flight and its associated research by Holden[1] demonstrates our present lack of predictive capability. Holden states that the intense research programs of the 1960s and early 1970s were superseded by hypersonic flow investigations that were limited to supporting specific missions such as the Space Shuttle, the Jovian entry vehicle, and ballistic re-entry vehicles. The results of this review vividly point out the scarcity of previous research encompassing the combined effects of surface roughness, turbulent boundary-layer separation, and hypersonic flows. Only one document, a final report by Holden,[2] has been identified as complementary to the present work. Holden's study examined control flap effectiveness in a separted high-speed flow, conditioned by surface proturbances. This preliminary work, however, does not provide any firm predictive analysis defining a rigorous correlation for nonsmooth surface effects on turbulent boundary-layer separation, thus, pointing out the void that exists.

Many earlier studies[3–8] on turbulent boundary-layer separation were performed on smooth surfaces in supersonic-hypersonic flow regimes. These studies investigated incipient separation using compression corners to simulate flow over aerodynamic flaps or ailerons.

Investigations addressing the effects of surface roughness on turbulent boundary-layer profiles and skin friction carried out by Goddard[9] demonstrated that surface imperfections, on a nonsmooth plate and of a height greater than the viscous sublayer, produce increases in the skin friction. Additionally, the inner portion of the boundary layer is shown to decrease under similar conditions. This experimental work has been consistently endorsed by other researchers that followed. Namely, Young,[10] Reda et al.,[11] and Thompson[12] all were in accord with Goddard's initial finding for Mach numbers up to 5.0. The latest work on the turbulent boundary-layer profile/skin friction and its dependence on surface roughness in a two-dimensional flow is that from Fiore and Christoph[13] at a Mach number of 5.75 and a Reynolds number of 34.5 × 10^6/m. They found that the rough surface velocity profile is less full than the velocity profile for the smooth wall case. The decrease in the local velocity, for the rough surface situation, is believed to be caused by the momentum loss resulting from the presence of pressure drag and a wake for the individual protuberances. Because high-speed flight vehicles exhibit a variety of nonsmooth surface conditions and employ various external control devices that can produce large areas of flow separation, the importance of understanding surface roughness effects on boundary-layer separation becomes very evident.

Facility

This investigation was carried out using the Air Force Flight Dynamics Laboratory's (FDL) High Reynolds Number Mach 6 Facility located at Wright-Patterson Air Force Base. This

Received May 13, 1989; presented as Paper 89-2163 at the AIAA 7th Applied Aerodynamics Conference, Seattle, WA, July 31–Aug. 2, 1989; revision received Aug. 9, 1990; accepted for publication Aug. 17, 1990.

*Associate Professor, Department of Aerospace Engineering, Mail Location 70. Member AIAA.
†Technical Manager. Senior Member AIAA.

wind tunnel is an open jet, blowdown facility. It is configured with a contoured axisymmetric nozzle having a 31.36-cm diam exit. Nozzle wall boundary-layer effects reduce the actual test core to a diameter of approximately 25.4 cm. Reservoir pressures range from 4.83 to 14.49 MPa at a reservoir temperature of approximately 517 K. These conditions correspond to freestream unit Reynolds numbers ranging from 33×10^6 to 98×10^6/m. Air storage capability allows for extended run times of up to 10 min. For further details of the Mach 6 Facility, see Fiore and Law.[14]

Model

An existing flat plate model with a rough surface typography was used in this experiment. This roughened surface is configured with milled proturbances measuring 0.508 mm in height and 1.016 mm for the lateral and streamwise widths (Fig. 1). The machined cavities separating the individual roughness elements in the cross stream and streamwise directions also measure 1.016 mm. Location of the beginning of the roughness pattern on the model was based on previous calculations performed by Shang.[15] This position was estimated to be 3.048 cm downstream of the leading edge where laminar-turbulent boundary-layer transition was expected to be completed. In addition to static pressures, wall temperatures were acquired using chromel/alumel thermocouples embedded in the plate surface adjacent to the pressure ports (Fig. 2).

The model was designed to extend the full width across the wind tunnel's open jet; however, the instrumented portion of the flat plate was only 10.16-cm wide and well within the test

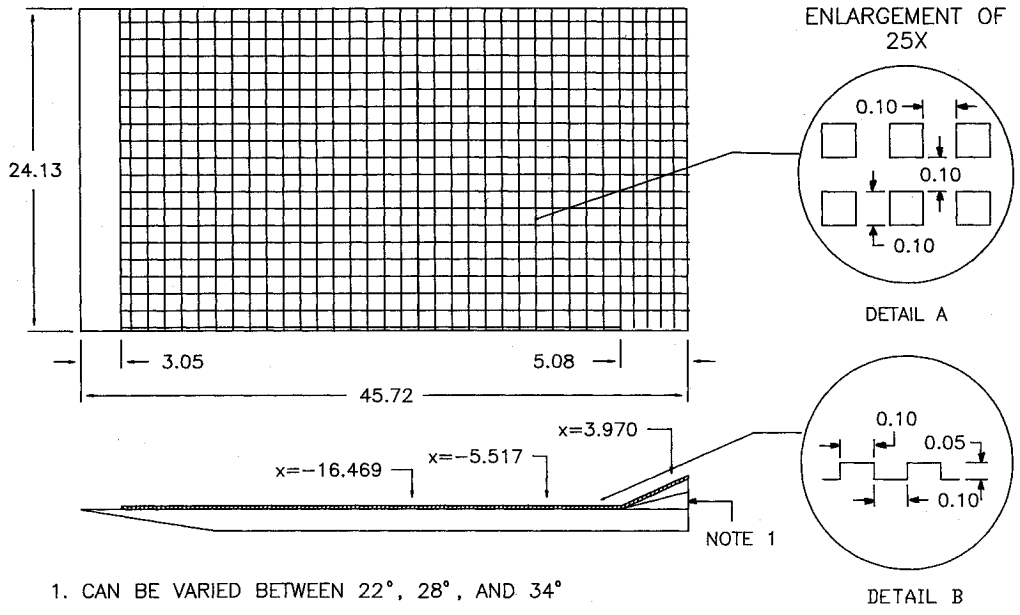

Fig. 1 Schematic of the flat plate ramp roughness geometry.

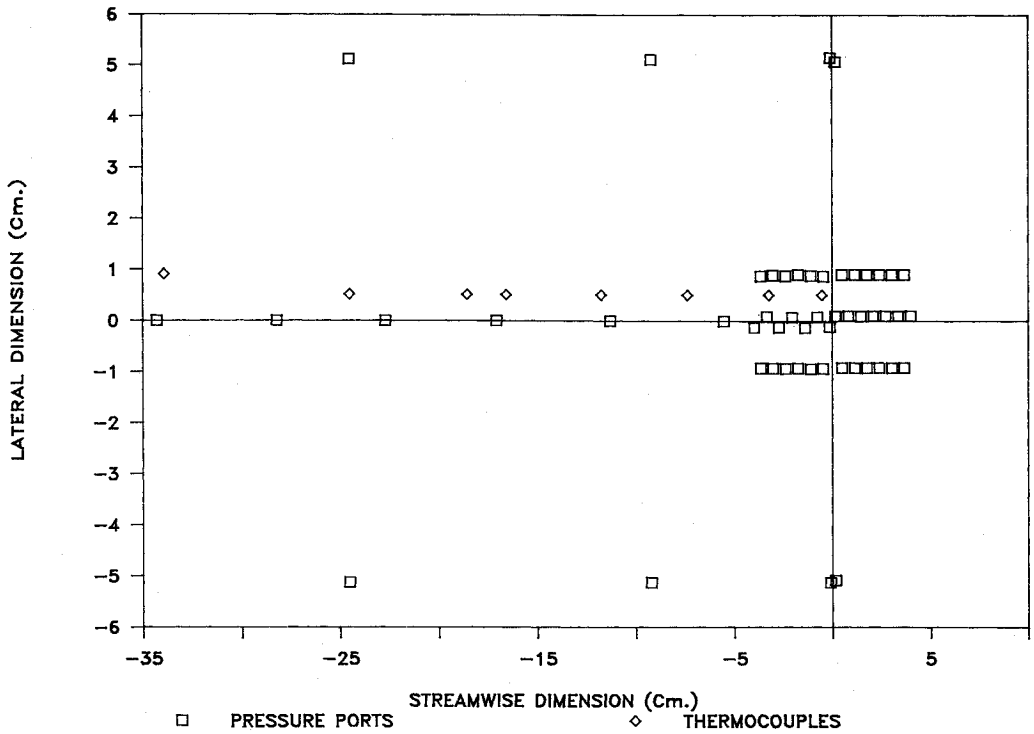

Fig. 2 Instrumented section of flat plate ramp.

core of the exiting jet. The plate's length is 46.99 cm and features a sharp 10-deg asymmetric leading edge.

Interchangeable wedges mounted at the model's trailing edge provided the necessary adverse pressure gradient for flow separation near the ramp intersection point. Three wedges, configured to angles of 22, 28, and 34 deg, were used. In the present paper only the 22-deg ramp results will be examined.

Experiment

All tests were performed at a nominal Mach number of 6 over a freestream unit Reynolds number range of 33×10^6 to 98×10^6/m. These high unit Reynolds numbers ensured the existence of a turbulent boundary layer within a few centimeters downstream of the leading edge. The resulting boundary layer was measured along the streamwise centerline of the model -16.469, -5.517, and $+3.970$ cm from the wedge/plate intersection point. Measurement was achieved by traversing pitot pressure and total temperature probes normal to the model surface. Corresponding wall temperatures and surface static pressures were measured and utilized for determining the velocity distribution within the shear layer upstream of the ramp/plate intersection point. For the location downstream of the ramp/plate intersection, the probe drive system was rotated in such a manner that the probe was aligned parallel to the inclined surface and enabled the traverses to be made normal to the wedge.

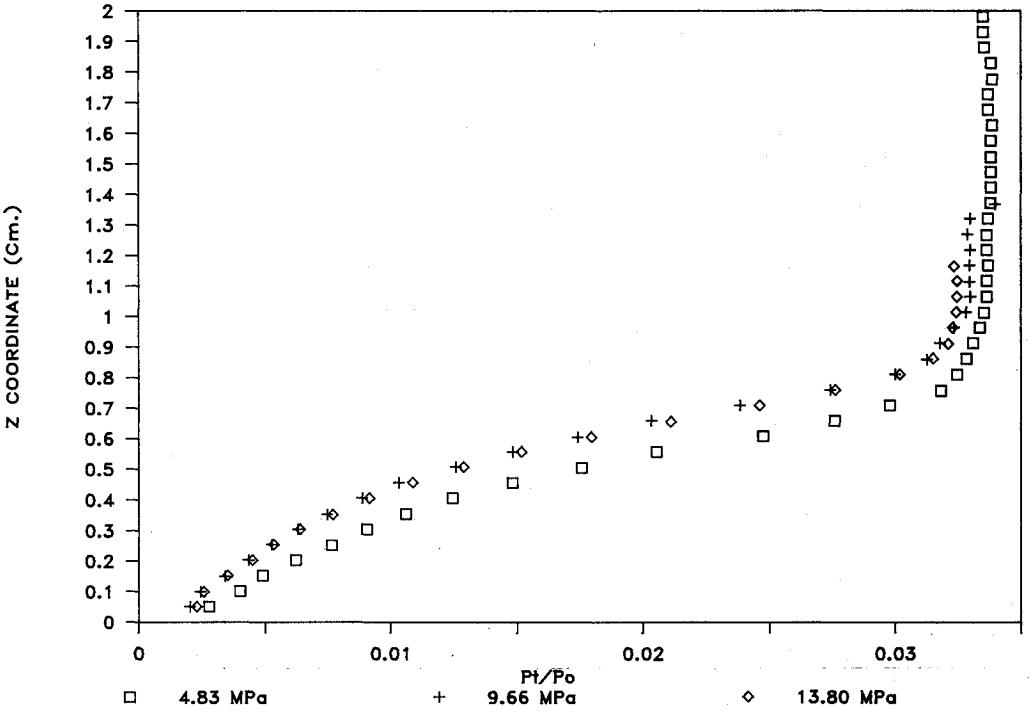

Fig. 3 Nondimensional pitot pressure distribution at $x = -5.517$ cm.

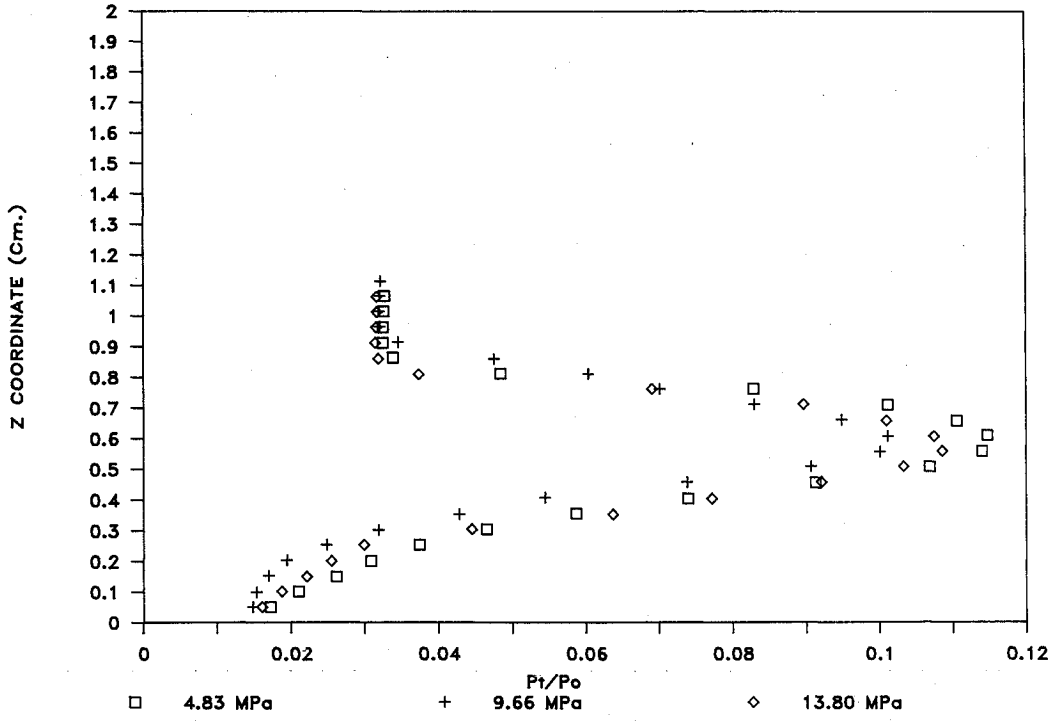

Fig. 4 Nondimensional pitot pressure distribution at $x = +3.970$ cm.

Measurement Uncertainties

Three basic parameters were measured in this experimental study: pressures, temperatures, and probe locations. The uncertainty in the pressure measurements is ±0.5% of the full-scale range of the transducer being used. For the reservoir pressure the uncertainty is ±103.4 KPa. For the pitot pressures the uncertainty is ±0.862 KPa for pressures below 172.4 KPa, and ±2.586 KPa for pressures equal to or greater than 172.4 KPa. For the surface pressures the uncertainty is ±0.862 KPa.

The uncertainty in the temperature measurements is based on the manufacturer's specifications of the particular type of standard thermocouple being used, since the calibration of the actual sensor is not done. For these studies the uncertainty in the temperature measurement is ±2.2 K.

The uncertainty in the probe location is somewhat difficult to estimate since the temperature of the model and the probe strut assembly were allowed to approach a stable temperature before the data were taken and the surface of the model was used to reference the probe position for each profile measurement. However, even with all this care the uncertainty of the probe position was estimated to be ±0.25 mm.

Results

In the present work, boundary-layer characteristics were determined from the total and static flow conditions acquired at three streamwise measurement locations. Two of the measurement locations, at $x = -16.469$ cm and $x = -5.517$ cm, were upstream of the plate/wedge intersection, and the third location on the ramp (or wedge) was at $+3.970$ cm downstream of the intersection point. By traversing a pressure probe through the boundary layer, the total pressure distribution was obtained for each of the three reservoir pressures tested. These reservoir pressures (4.83, 9.66, and 13.80 MPa) corresponded to approximate unit Reynolds numbers of 33×10^6, 66×10^6, and 98×10^6/m, respectively. The total pressure traverses obtained at $x = -5.517$ cm and $+3.970$ cm were nondimensionalized by the stagnation pressure P_0 and plotted in Figs. 3 and 4, respectively. Also, a comparison of the total pressure profiles obtained at the three stations is examined (Fig. 5) for a constant P_0 (4.83 MPa) or unit Re (33×10^6/m).

Surface (static) pressures were recorded for the flat plate/22-deg ramp combination. These surfaces pressures P_i were normalized by the undisturbed static pressure P_{ref} obtained upstream of the interaction zone at $x = -16.469$ cm (Figs. 6 and 7). Comparisons of P_i/P_{ref} obtained on a smooth surface model under the same flow conditions are plotted along with the rough surface pressure distribution in Figs. 8a and 8b.

Utilizing the assumption that the static pressure through the boundary layer is constant upstream of the interaction region, the Mach number distributions were calculated for all cases except those at $x = +3.970$ cm. That is, using the Rayleigh pitot equation for the pressure ratio P_t/P_s the Mach number distribution throughout the boundary layer was calculated. Figure 9 is an example of such profiles obtained at $x = -5.517$ cm for the three reservoir pressures tested. Total temperature traverses at each measurement station were also acquired for each of the three reservoir pressures. All total temperature T_t measurements acquired were nondimensionalized by the reservoir temperature T_0. These temperature ratio profiles T_t/T_0 were obtained at $x = -5.517$ and $+3.970$ cm and are plotted in Figs. 10 and 11 for $P_0 = 4.83$, 9.66, and 13.8 MPa, respectively. Similarly, Fig. 12 is a comparison of the temperature ratios acquired for $P_0 = 4.83$ MPa (or unit $Re \simeq 33 \times 10^6$/m) for the three streamwise measurement stations. Using the adiabatic relation between Mach number and temperature ratio (T_s/T_t), the static temperatures T_s throughout the boundary layer at $x = -5.517$ cm were calculated. Once the value of T_s was determined, the local speed of sound c was calculated and, hence, the local mean velocity was determined at $x = -5.517$ cm (Fig. 13). The present boundary-layer velocity distribution was then compared (Fig. 14) to both the 1/7 power law profile and the velocity profile obtained using the Van Driest velocity transformation.[16]

Discussion

In this investigation the detailed documentation of the boundary-layer characteristics was obtained both upstream and downstream of the ramp intersection point. Figures 3 and 4 appear to indicate a fuller pitot pressure profile for the lowest unit Re case ($P_0 = 4.83$ MPa). Convergence to the

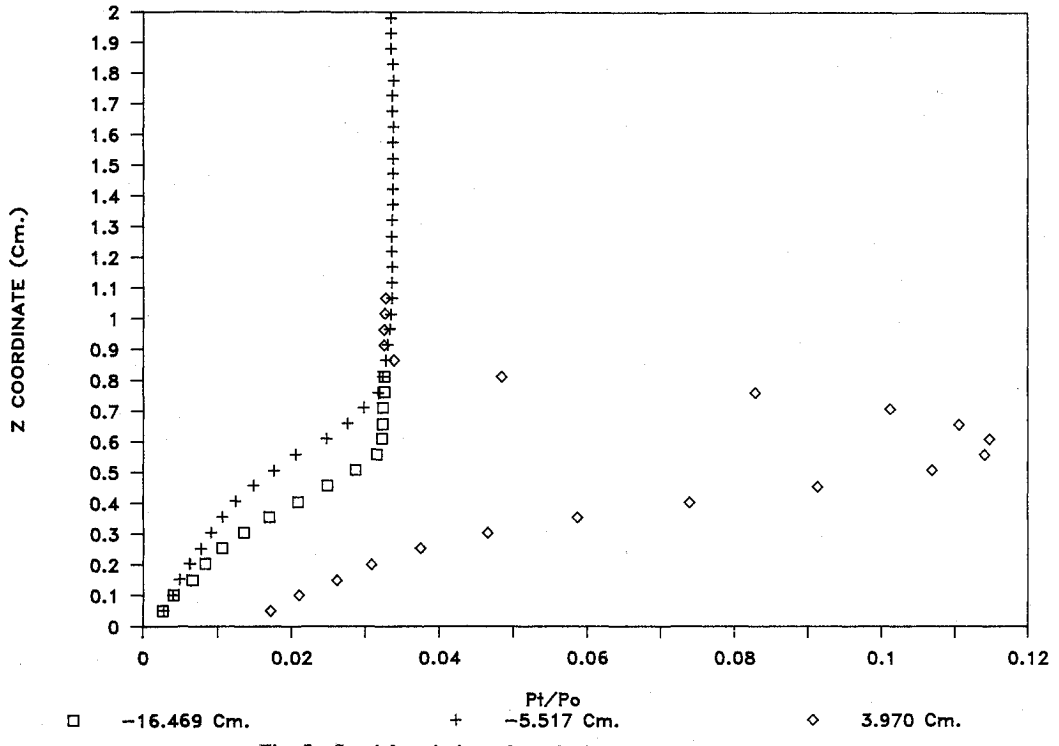

Fig. 5 Spatial variation of the $P_t/P_0 = 4.83$ MPa.

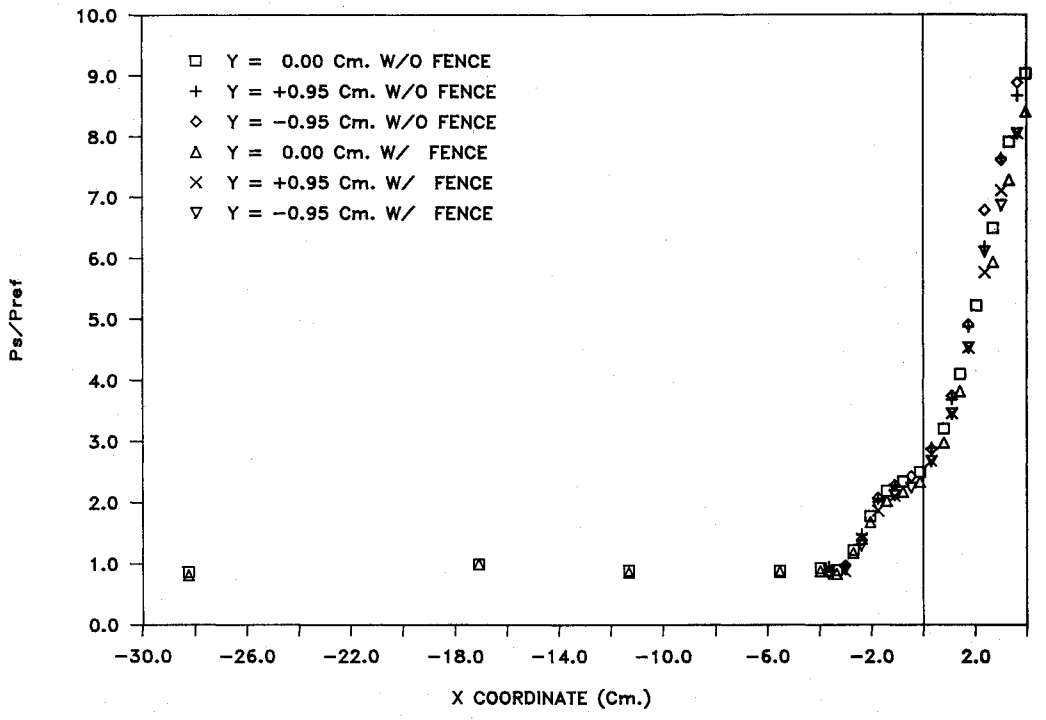

Fig. 6 Nondimensional streamwise surface pressure distribution at P_0 = 4.83 MPa with and without a fence.

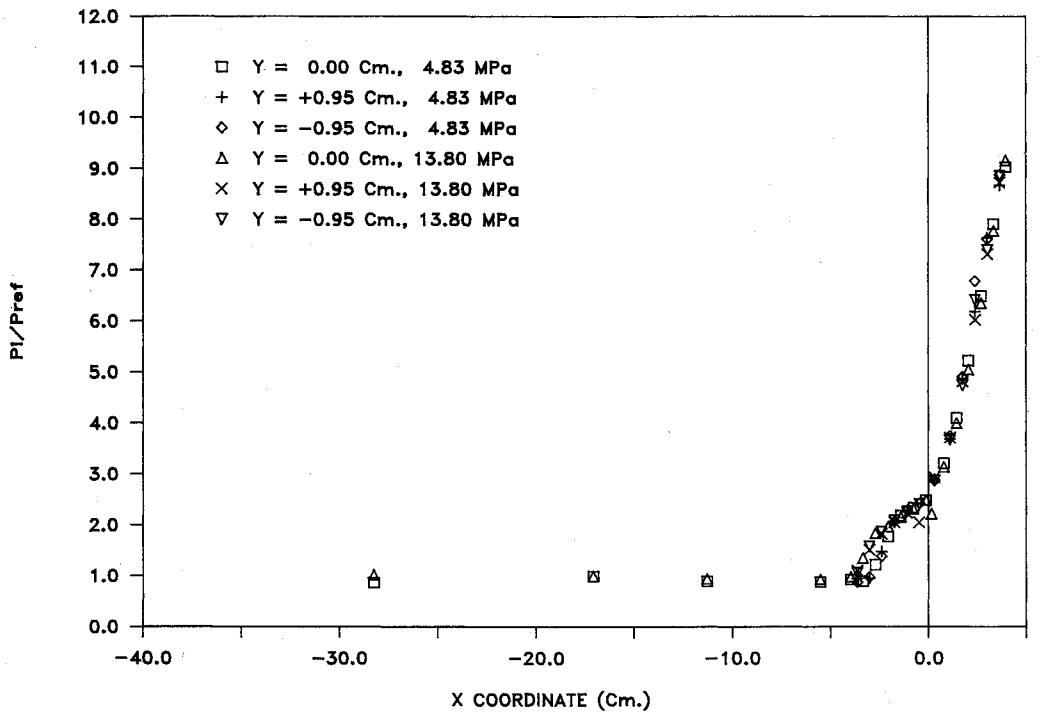

Fig. 7 Nondimensional streamwise surface pressure distribution for P_0 = 4.83 MPa and 13.80 MPa.

freestream values at each of the measurement locations for the different *Re* cases tested indicate that for the P_0 = 4.83 MPa and 9.66 MPa runs, the P_t/P_0 ratio appears to be several percent higher than the high *Re* case (P_0 = 13.8 MPa). Although convergence to an approximately constant freestream pitot pressure was found, in Fig. 5 the pitot pressure ratio on the ramp was observed to exhibit a completely different behavior. Specifically, before reaching the freestream ratio a sizable peak in the pressure profiles were recorded. The magnitude of this peak is approximately 3.5 times greater than the P_t/P_0 ratio observed at location upstream of the 22-deg ramp. This is a result of the local shock structure in the reattachment region.

Utilizing inviscid oblique shock wave theory one is able to calculate a shock angle of 31 deg. Based on a freestream Mach number of 5.9, the pressure ratio was estimated to be 3.1. This value differed approximately 11% from the experimentally determined pressure ratio of 3.5. Therefore, if appears that the combined efforts of viscosity and roughness are small. Furthermore, using the experimentally determined pressure ratio and calculating the shock angle from the normal shock tables[17] an angle of 32.27 deg is obtained.

An examination of the surface pressure distribution in Figs. 6 and 7 clearly indicates the two-dimensional nature of the flow. From a comparison of surface pressures obtained at y =

0 and $y = \pm 9.14$ cm (Fig. 6), it can be concluded that excellent agreement exists over the center portion of the plate through the interaction zone. To further verify the two dimensionality of the flow, side fences were added to the model. No notable difference in the surface pressure was observed. If one assumes the position of the inflection point in the surface pressure distribution (Fig. 7) to be the location of separation point x_s, then x_s can be estimated in the present study to be approximately 22.86 mm upstream of the plate/ramp intersection point in the low *Re* case and approximately 25.4 mm upstream for the high *Re* case. While difficult to measure, the extent of separation appears to be identical for Reynolds numbers approximately greater than 66×10^6/m. Also, the pressures on the ramp surface appear to coincide for both cases indicating approximately the same location for the reattachment point.

Comparisons made to the smooth surface study[18] (with a 22-deg compression corner) indicated the extent of separation was an order of magnitude larger in the rough surface study (Figs. 8a and 8b). That is, on the rough surface model, the upstream location of the separation point was 10 times greater for the low unit Reynolds number case (Fig. 11a) and 12 times greater for the high unit *Re* case (Fig. 11b).

The Mach number distribution as a function of distance z away from the wall for the three *Re* tested is plotted in Fig. 9. From this figure it appears that the indicated freestream Mach

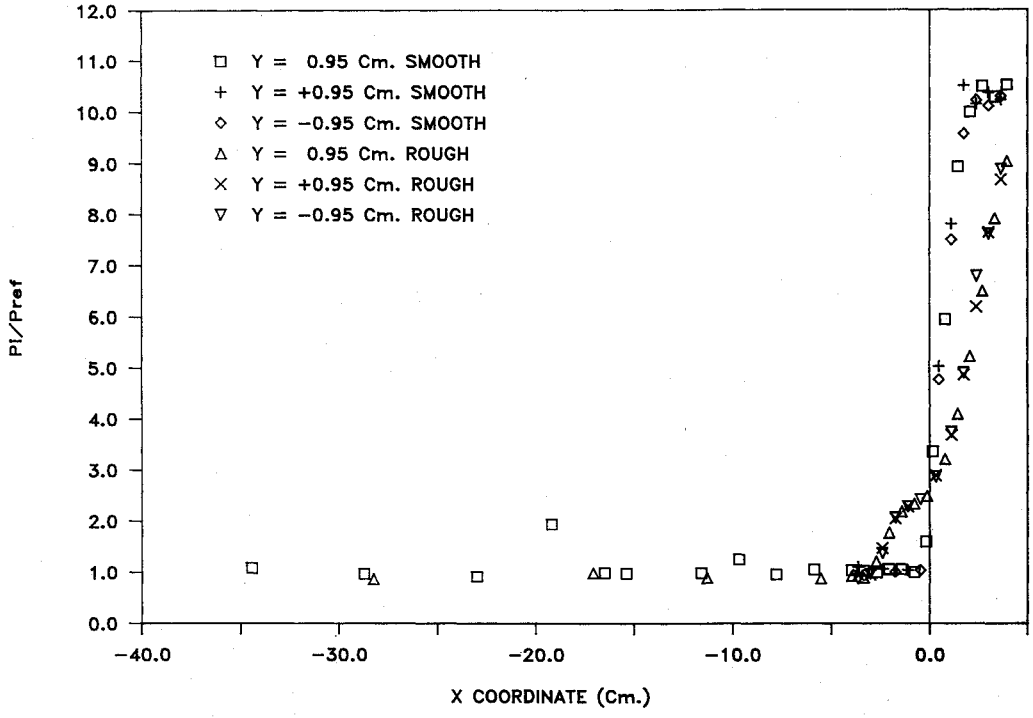

Fig. 8a Surface pressure comparison between rough and smooth geometry at $P_0 = 4.83$ MPa.

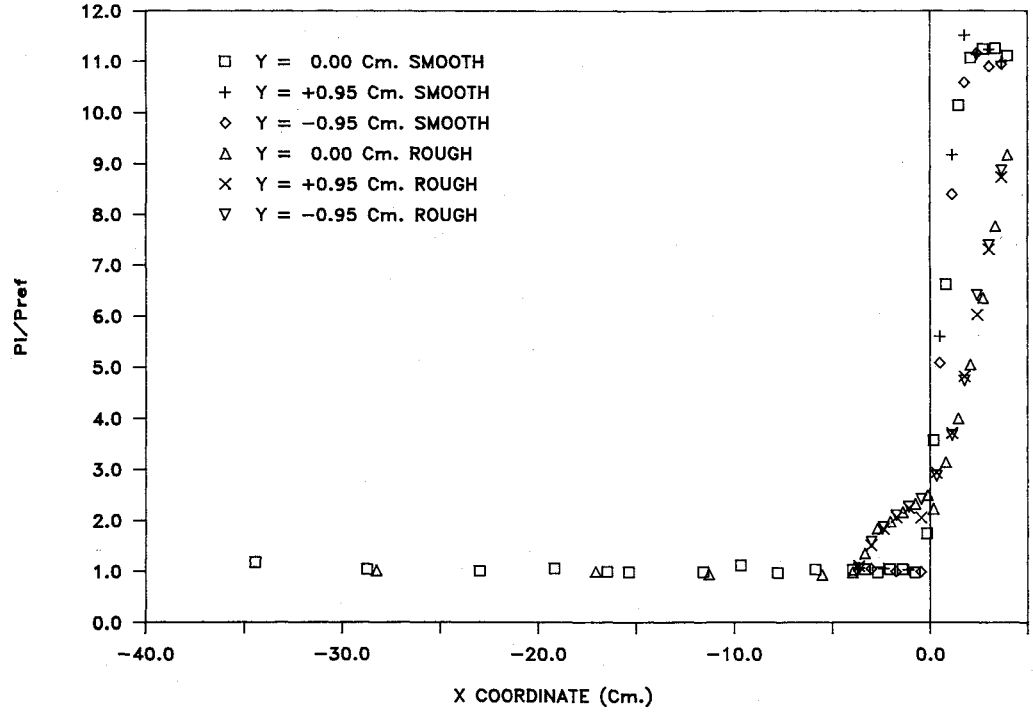

Fig. 8b Surface pressure comparison between rough and smooth geometry at $P_0 = 13.80$ MPa.

number for all three cases is approximately 5.9. In addition, it appears to suggest that the boundary-layer thicknesses for the low and intermediate *Re* cases are approximately the same for the streamwise position $x = -5.517$ cm (upstream from the separation point). Although one would expect a thinning of the boundary layer as the *Re* was increased, this effect was offset to some extent by the forward movement of the separation point.

An examination of Fig. 10 shows that the total temperature profiles obtained at $x = -5.517$ cm were similar for all three *Re* tested. Specifically, a 3–5% overshoot in the T_t profiles has been observed at this location in the present work. This increase in T_t is a result of the combined viscous and turbulent shear stresses in the outer portion of the boundary layer doing work on the fluid to increase its internal energy, hence, increasing the temperature of the fluid in the inner region of the boundary layer. The total temperature on the ramp (Fig. 11) was also found to exceed T_0, by 20% for the lowest *Re* case and approximately 30% in the highest *Re* case. In addition, a bimodal character was observed, that is, there was a second temperature maximum in the total temperature profiles. This second overshoot in total temperature was between 5 and

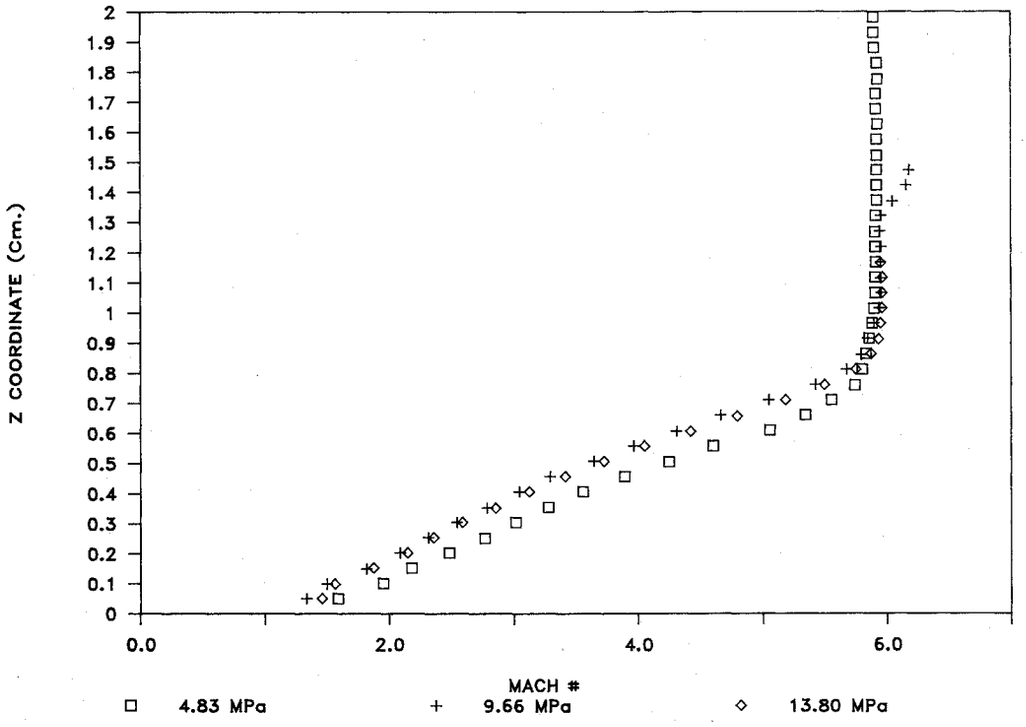

Fig. 9 Mach number profiles at $x = -5.517$ cm.

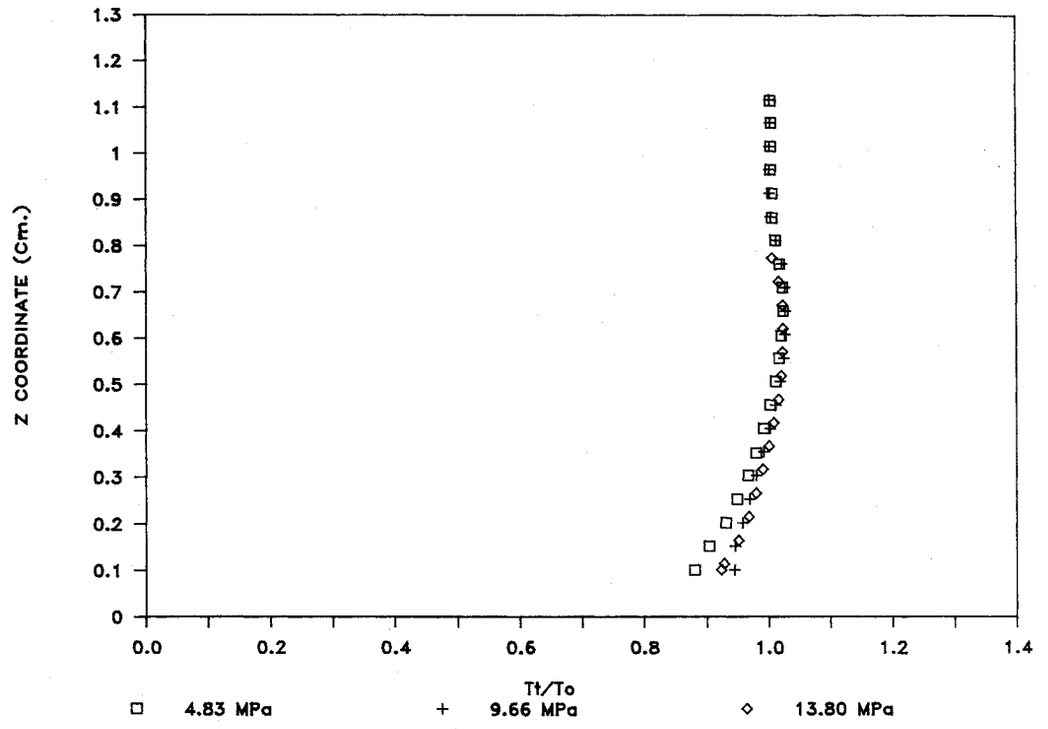

Fig. 10 Nondimensional total temperature profiles at $x = -5.517$ cm.

15%. Inspection of Fig. 12 shows that for a constant unit *Re* the maximum T_t recorded at stations upstream of the ramp were found to have the same level of overshoot and reduced to the freestream total temperature within a couple of percent. As previously stated, the profile obtained on the ramp ($x = +3.970$ cm) indicated a bimodal character, overshooting T_0 by a minimum of 5 and 20% before convergence to a final value, approximately 4% under the freestream T_0.

Similar features can be found in the mean velocity and turbulent intensity measurements obtained by Maurice and Seibert[9] on the same model using laser velocimetry (LV). An examination of their mean velocity profiles obtained upstream of the compression corner indicates a developed turbulent velocity profile. As will be shown later, these LV profiles are in good agreement with the present profiles collected from pressure and temperature probe data. Also, LV measurements of the turbulent intensity indicate values of the streamwise component approaching 13% near the wall. Comparing turbulence intensity profiles obtained on the ramp to those upstream indicates the presence of a second peak. That is, at

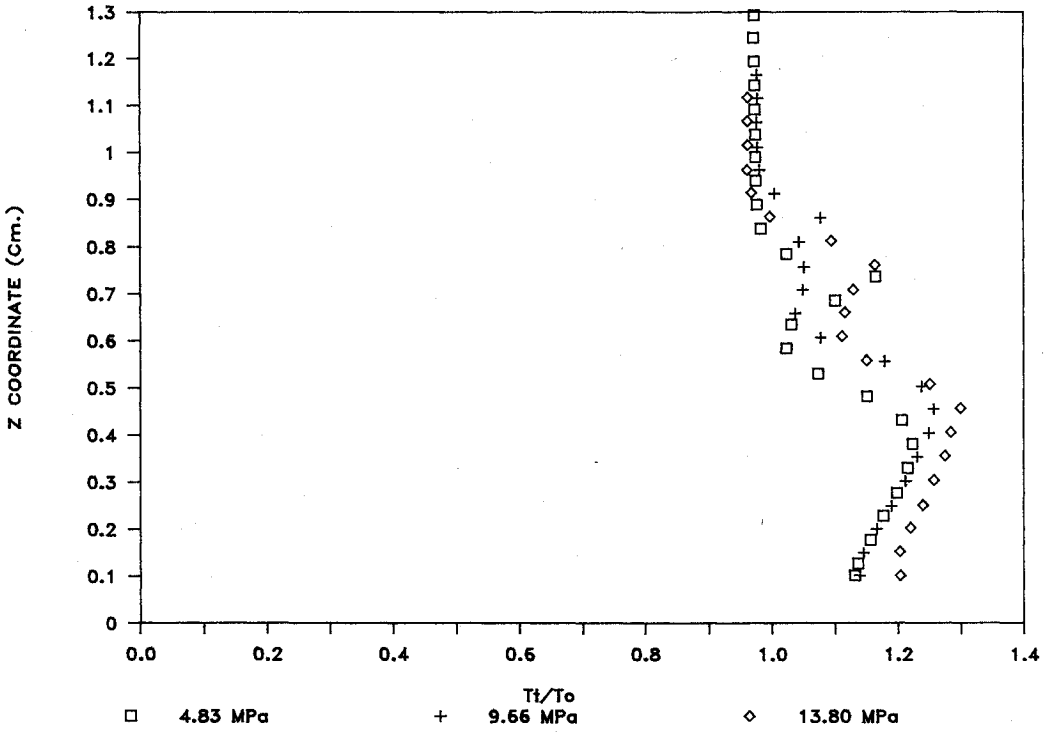

Fig. 11 Nondimensional total temperature profiles at $x = +3.970$ cm.

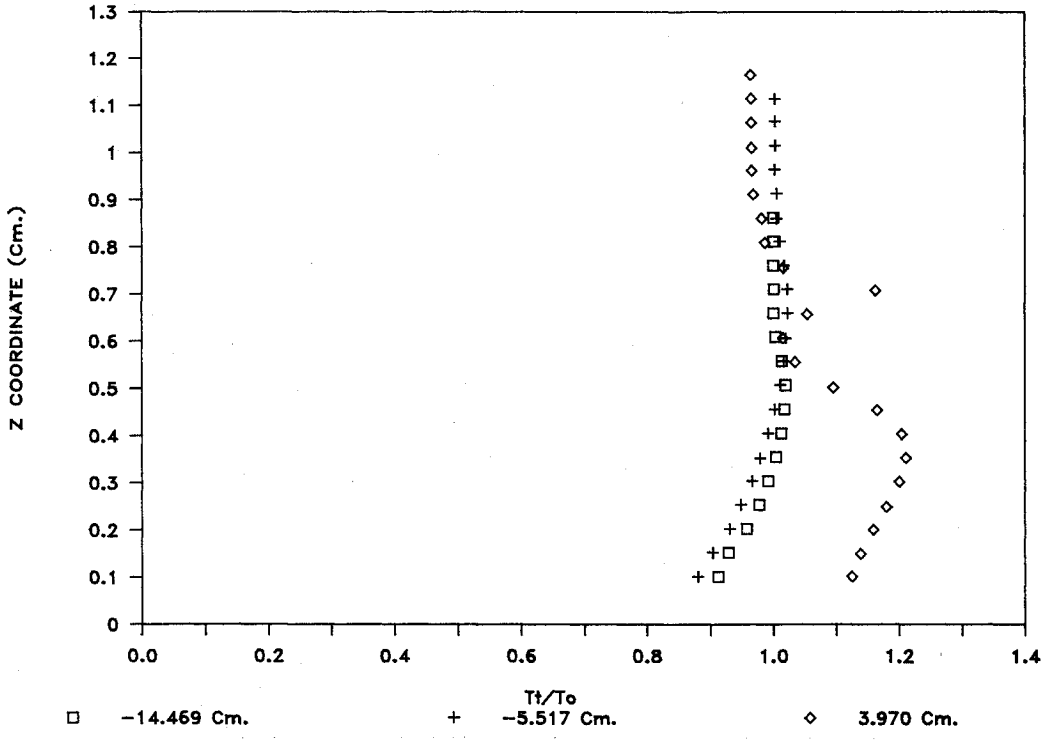

Fig. 12 Spatial variation of the T_t/T_0 ratio for $P_0 = 4.83$ MPa.

$z/\delta = 0.308$ and 0.615 the turbulence intensity was measured to be 0.17 and 0.23, respectively. In addition, a freestream value of 0.019 was recorded at $z/\delta = 1.19$.

A re-examination of the T_t profiles indicates a strong T_t peak at $z/\delta = 0.62$, with a second, weaker peak at $z/\delta = 1.16$. This narrow second T_t peak appears just at the edge of the boundary layer and at a point of minimum turbulence. This peak can be associated with the unsteadiness in the shock position. That is, as the separating shock structure moves, so does the boundary-layer edge. If one takes a closer look at the streamwise component of turbulent intensity data, from $z/\delta = 0.85$ to 1.19 the magnitude was found to only vary by approximately 40%. It is in this outer region between $z/\delta = 0.85$ and 1.19 where the movement of the boundary layer causes an extension of the large-scale mixing region and a local redistribution of energy (a second T_t peak). Moving into the region of a stable boundary-layer edge structure (below $z/\delta = 0.85$) the streamwise component of turbulent intensity was observed to jump by approximately 500% at $z/\delta = 0.615$. Furthermore, the turbulent intensity variation in this region was determined to be less than 35%. It is important to note that at $z/\delta \simeq 0.62$, both the turbulent intensity and T_t reach a maximum. Hence, it appears to support the idea that the turbulent stresses extract energy from the flow that locally heats the fluid and produces the observed primary T_t peak.

Further support for the multiple T_t peaks was found from measurements obtained on a 24-deg ramp at Mach 2.84 and a unit Reynolds number of 65×10^6/m by Seleg et al.[20] Using

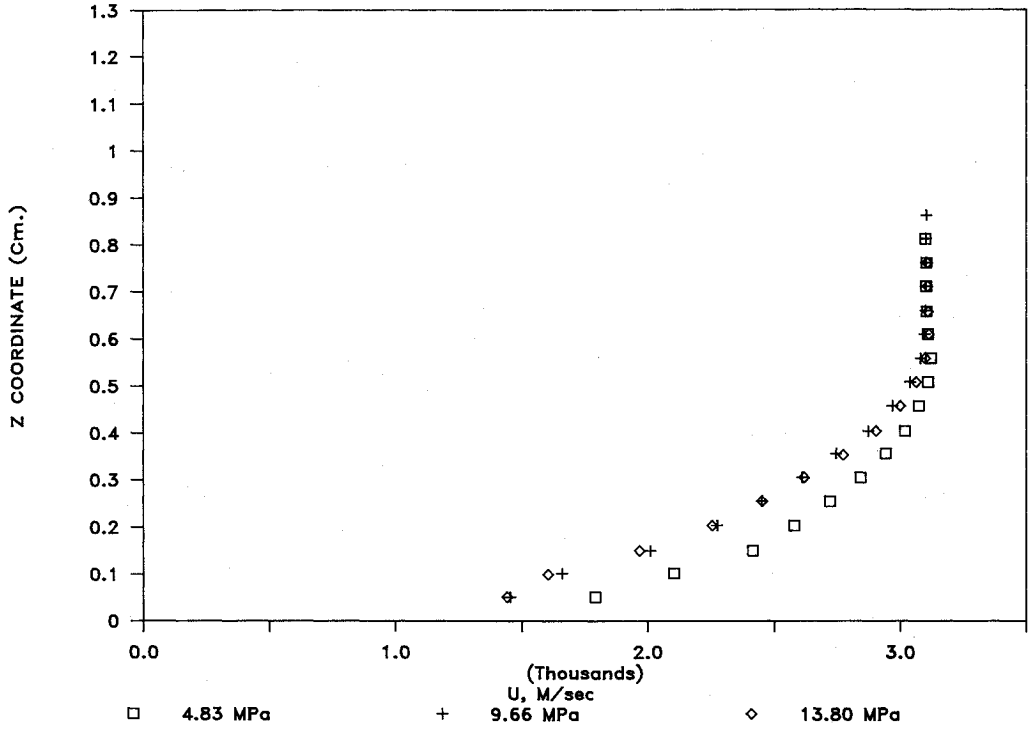

Fig. 13 Velocity profiles at $x = -5.517$ cm.

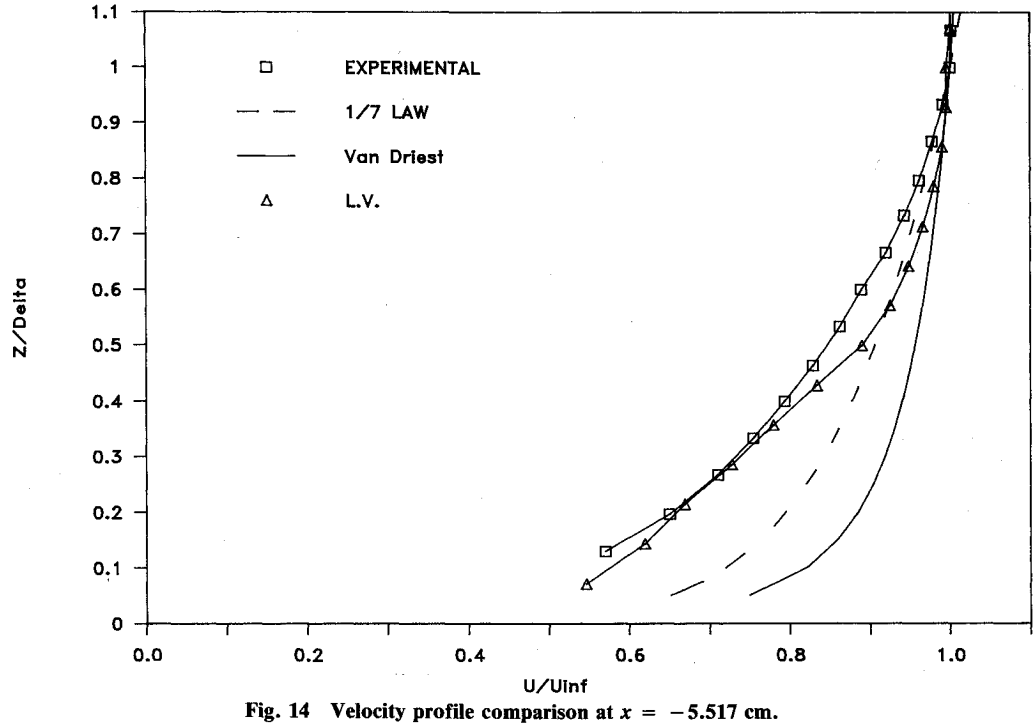

Fig. 14 Velocity profile comparison at $x = -5.517$ cm.

hot-wire anemometry, bimodal mass flux probability density functions were recorded on the ramp, and a single maximum at upstream measurement stations. That is, the mass flux turbulence intensity profiles acquired on the ramp were also determined to have multiple peaks. Comparing the ramp turbulence intensity profiles to those obtained upstream of the ramp intersection indicated an increase by a factor of five.

The mean velocity distribution (calculated from the pressure and temperature probe data) obtained upstream of the plate/ramp intersection point at $x = -5.517$ cm is shown in Fig. 13. Although some spread in the velocity data was found close to the wall, all tests appear to converge to a freestream velocity of approximately 950 m/s $\pm 0.3\%$. Also, Fig. 14 indicates the deviation of the experimental data from both the 1/7 power law formulation and the Van Driest velocity transformation. In addition, for the purpose of comparison the LV data is included. Agreement between experimentally determined velocity techniques was of the order of 5%. The lack of fullness of the experimental velocity profiles near the wall is believed to be a result of the momentum loss in the boundary-layer flow. It is felt that this loss momentum is a direct result of the shocklets and wakes produced by the individual roughness elements.

Summary

An experimental investigation into rough surface turbulent boundary-layer characteristics at hypersonic speeds has been undertaken. These experiments were carried out on a rough flat plate/wedge combination at a nominal Mach number of 6 for unit Reynolds numbers between approximately 33×10^6 and 98×10^6/m. The roughened surface geometry consists of machined proturbances 0.508 mm high and 1.016 mm in both length and width, with spacing between the individual elements of 1.016 mm.

The results of the surface pressure distributions indicate a two-dimensional flow over the model. To further assure and verify two-dimensionality, fences were added to the model surface at the intersection region. Comparison of the surface pressure distributions with and without the fences proved to be excellent. Using the first inflection point in the surface pressure distribution as an indication of separation, the extent of separation x_s was determined. It was estimated that the separation point moved upstream by approximately 10% as the unit Re was increased from 33×10^6 to 98×10^6/m. However, for the smooth surface case, the separation distance did not change as the Re was increased from 33×10^6 to 98×10^6/m. Yet, when compared to the smooth surface case, the separation distance for the rough surface case was found to be 10–12 times larger.

Pitot pressure profiles obtained perpendicular to the ramp surface reached levels 3.5 times greater than the freestream pitot pressure. Total temperature profiles also acquired perpendicular to the ramp surface indicated a bimodal character. This double maximum was determined to exceed the stagnation temperature by 5–30%. It is proposed that the weaker second peak is a manifestation of the boundary-layer edge movement, and the primary T_t peak a result of the high level of turbulence which was found to exist in the boundary layer at the same location.

A comparison of the experimentally determined velocity profiles to those calculated using both the 1/7th power law form and the Van Driest velocity transformation was performed. These results indicated that the experimentally obtained velocity profiles were not as full near the wall, representing a reduction in momentum. This momentum loss is believed to be a result of the viscous/turbulent dissipation resulting from the rough surface. That is, this loss is a result of the shocklets and wakes produced on and by the individual roughness elements.

Acknowledgment

This project was sponsored by the United States Air Force Office of Scientific Services, Bolling AFB, Washington, DC, and the Flight Dynamics Laboratory, Wright-Patterson AFB.

References

[1]Holden, M. S., "A Review of Aerothermal Problems Associated with Hypersonic Flight," AIAA Paper 86-0267, Jan. 1986.

[2]Holden, M. S., "Studies of Boundary Layer Transition and Surface Roughness Effects in Hypersonic Flow," Air Force Office of Scientific Research, Bolling AFB, Washington, DC, Final Rept. 6430-A-5, Oct. 1983.

[3]Bogdonoff, S. M., Vas, I. E., Settles, G. S., and Simper, G., "Research on Turbulent Separated and Reattached Flows," Aerospace Research Lab., Wright-Patterson AFB, Dayton, OH, ARL 75-0220, June 1975.

[4]Kuehn, D. M, "Turbulent Boundary-Layer Separation Induced by Flares on Cylinders at Zero Angle of Attack," NASA TR R-117, 1961.

[5]Kuehn, D. M., "Experimental Investigation of the Pressure Rise Required for the Incipient Separation of Turbulent Boundary Layers in Two-Dimensional Supersonic Flow," NASA Memo 1-21-59A, Feb. 1959.

[6]Roshko, A., and Thomke, G. J., "Supersonic, Turbulent Boundary-Layer Interaction with a Compression Corner at Very High Reynolds Number," *Proceedings of the 1969 Symposium on Viscous Interaction Phenomena in Supersonic and Hypersonic Flow,* Univ. of Dayton Press, Dayton, OH, 1969, pp. 109–138.

[7]Sterrett, J. R., and Emery, J. C., "Experimental Separation Studies for Two-Dimensional Wedges and Curved Surfaces at Mach Numbers of 4.8 to 6.2," NASA TN D-1014, Feb. 1962.

[8]Todisco, A., and Reeves, B. L., "Turbulent Boundary Layer Separation and Reattachment at Supersonic and Hypersonic Speeds," *Proceedings of the 1969 Symposium on Viscous Interaction Phenomena in Supersonic and Hypersonic Flow,* Univ. of Dayton Press, Dayton, OH, May 1969, pp. 139–179.

[9]Goddard, F. E., Jr., "Effect of Uniformly Distributed Roughness on Turbulent Skin-Friction Drag at Supersonic Speeds," *Journal of the Aero/Space Sciences,* Vol. 26, Jan. 1959, pp. 1–15.

[10]Young, F. L., "Experimental Investigation of the Effects of Surface Roughness in Compressible Turbulent Boundary Layer Skin Friction and Heat Transfer," Defense Research Lab., Univ. of Texas at Austin, Rept. DRL-532, May 1965.

[11]Reda, D. C., Ketter, F. C., Jr., and Fan, C., "Compressible Turbulent Skin Friction on Rough and Rough/Wavy Walls," *AIAA Journal,* Vol. 13, No. 5, 1975, pp. 533–554.

[12]Thompson, M. J., "Skin Friction and Heat Transfer in Turbulent Boundary Layers as Influenced by Roughness," Applied Research Lab., Johns Hopkins Univ., Baltimore, MD, Rept. ARL-TR-70-43, Dec. 1970.

[13]Christoph, G. H., and Fiore, A. W., "Numerical Simulations of Flow Over Rough Surfaces, Including Effects of Shock Waves," Flight Dynamics Lab., Wright-Patterson AFB, Dayton, OH, Final Rept. AFWAL-TR-83-3071, Aug. 1983.

[14]Fiore, A. W., and Law, C. H., "Aerodynamic Calibration of the Aerospace Research Laboratories M-6 High Reynolds Number Facility," Aerospace Research Lab., Wright-Patterson AFB, Dayton, OH, Final Rept. ARL TR 75-0028, Feb. 1975.

[15]Shang, J. S., Hankey, W. L., and Dyer, D. L., "Compressible Turbulent Boundary Solutions Employing Eddy Viscosity Models," Aerospace Research Lab., Wright-Patterson AFB, Dayton, OH, Rept. ARL-73-0041, March 1973.

[16]Van Driest, E. R., "Turbulent Boundary Layer in Compressible Fluids," *Journal of the Aero/Space Sciences,* Vol. 18, March 1951, pp. 145–160.

[17]NACA, "Equations, Tables, and Charts for Compressible Flow," NACA Rept. 1135, 1953.

[18]Disimile, P. J., and Scaggs, N. E., "The Effect of Wedge-Induced Separation on Turbulent Boundary Layer Characteristics Over a Smooth Surface at Mach 6," AIAA Paper 90-3028, Aug. 1990.

[19]Maurice, M. S., and Seibert, G. L., "The LV Measured Turbulent Structure of Mach 6 Flow over a Roughened Flat Plate with a Compression Ramp," AIAA Paper 89-2164, July 1989.

[20]Sely, M. S., Andreopoulos, J., Muck, K. C., Dussauge, J. P., and Smits, A. J., "Turbulence Structure in a Shock Wave/Turbulent Boundary-Layer Interaction," *AIAA Journal,* Vol. 27, No. 7, 1989, pp. 862–869.

Clark H. Lewis
Associate Editor